A New 2-D Image Reconstruction Algorithm Based on FDTD and Design Sensitivity Analysis

No-Weon Kang, Young-Seek Chung, *Member, IEEE*, Changyul Cheon, *Member, IEEE*, and Hyun-Kyo Jung, *Senior Member, IEEE*

***Abstract*—This paper proposes a numerical algorithm that reconstructs the complex permittivity profile of unknown scatterers by the design sensitivity analysis (DSA) and topology optimization technique. By introducing the DSA and adjoint-variable method, the derivatives of the error function with respect to the complex permittivity variables can be calculated, and the material property in each cell can be changed simultaneously using sensitivity information. The steepest descent method is used as an optimization technique. The proposed method is validated by applying it to reconstructions of unknown two-dimensional scatterers that are illuminated by TM^z with a Gaussian-pulsed plane wave.**

***Index Terms*—Design sensitivity analysis (DSA), finite-difference time-domain (FDTD) methods, inverse problems, topology optimization.**

I. Introduction

IMAGING OF the permittivity and conductivity profiles of unknown objects from a measured scattered electromagnetic field has been of interest to microwave engineers for many years. This is because it is considered to be fundamental and essential in microwave-imaging applications. Recently, the interest of microwave imaging has increased in fields such as biological application, and the key step for implementing microwave imaging is an efficient solution of the associated inverse-scattering problem.

The reconstruction of a complex permittivity profile in inhomogeneous structures can be considered to be an optimization problem to minimize the difference between the measured field data and calculated ones by controlling the complex dielectric permittivity in the test domain. Such a difference is defined as an error function that needs to be minimized. However, the inverse-scattering problems are known to have nonlinear and ill-posed properties due to the lack of the measured information and the multiscattering effects between the objects [1]. In order to effectively reconstruct the unknown profiles, the first-order method using the gradient information and an iterative technique has been preferred.

Manuscript received April 5, 2002. revised August 26, 2002. This work was supported in part by the Korean Ministry of Science and Technology under the Creative Research Initiative Program, Seoul, Korea.

N.-W. Kang and H.-K. Jung are with the School of Electrical Engineering, and Computer Science, Seoul National University, Seoul 151-742, Korea (e-mail: knw@ elecmech.snu.ac.kr).

Y.-S. Chung is with the Department of Electrical and Electronic and Computer Science, Syracuse University, Syracuse, NY 13244 USA (e-mail: ychung05@mailbox.syr.edu).

C. Cheon is with the Department of Electronics, University of Seoul, Seoul 130-743, Korea (e-mail: chanyul@uos.ac.kr).

Digital Object Identifier 10.1109/TMTT.2002.805294

Reformulation of the inverse problem as a nonlinear optimization one and its solution using various optimization methods has been suggested [2]–[11]. In most approaches, the direct scattering problem is treated by means of the method of moments (MoM) and the inverse techniques use gradient-based algorithms that minimize the appropriately chosen cost function [2]–[5]. In these approaches, the direct scattering problem solution is achieved either during each iteration or it is implemented iteratively within the cost-function minimization. Other approaches have introduced the use of the finite-element method (FEM) or its hybrid coupling with the boundary-element method (BEM), while the inversion is based on the conjugate-gradient [6] or Newton's [7] iterative schemes, respectively.

Inversion algorithms using the finite-difference time-domain (FDTD) technique have been developed by many researchers. Chew developed a time-domain approach in the distorted-Born iterative method to reconstruct the images [8]. This method has added the advantage of information for target recognition available from ultrawide-band illumination [9]. Hagness *et al.* suggest an algorithm for breast cancer detection using pulsed confocal microwave imaging [10], [11]. The unknown object is illuminated and the backscattered signal is recorded for a number of antenna positions. A time shift and add algorithm is applied to the set of recorded signals in order to enhance returns from the high-contrast objects and reduce clutter.

The concept of design sensitivity analysis (DSA) has been studied and presented in structural engineering [14], and the FEM approach of the inverse-scattering problem using a conjugate-gradient optimization technique and DSA has been suggested by Rekanos *et al.* [6]. Recently, an optimization method based on the FDTD and DSA in the time domain was proposed [12], [13]. The DSA concerns the relationship between the design goal (or the objective function) and the design variables. That is, the DSA is to evaluate the derivative of the objective function with respect to the design variables.

In this paper, a new reconstruction algorithm that uses the derivatives information calculated by the FDTD technique and DSA is proposed. The adjoint-variable method is adopted in order to effectively calculate the derivative information of the error function [14]. The adjoint-variable method can calculate the sensitivity of all inversion variables (i.e., complex permittivity variables) by only one solving process of the adjoint-variable equation. Each iteration of the proposed method requires two solving processes, i.e., one for the forward problem and the other for the adjoint equation to calculate the sensitivity of each complex permittivity variable. Therefore, our algorithm needs

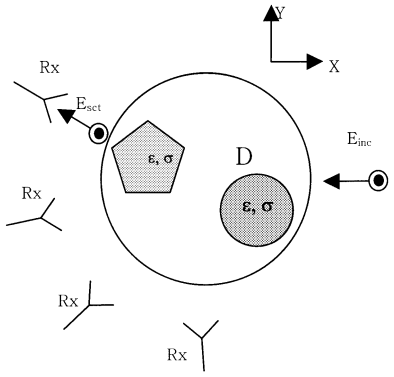

Fig. 1. 2-D inverse scattering problem for dielectric cylinders. D is the objective domain to be reconstructed. $E_{\rm inc}$ denotes the incident electric field intensity, $E_{\rm sct}$ denotes the scattered electric-field intensity, and Rx denotes the receiving antenna. The incident wave is assumed to be a plane wave.

roughly twice the CPU time compared to the normal FDTD forward analysis. In addition, the characteristics of the convergence can be improved by introducing the topology optimization based on normalized material density [15].

To demonstrate the validity of the method, the image reconstruction algorithm is applied to reconstruct the unknown two-dimensional (2-D) scatterers that are illuminated by TM^z with a Gaussian-pulsed plane wave. As a numerical example, the lossy object surrounded by air or the lossy medium, which has a relatively high permittivity, was reconstructed. Furthermore, multiple objects that are immersed in the lossy medium were reconstructed. In these numerical examples, the dispersive property of the permittivity and conductivity was not considered. The objective function was defined as the square of the error between the measured scattered electric and calculated fields.

The total-field/scattered-field technique was introduced in order to realize a plane-wave source [16]. To reduce the computational domain, Berenger's perfectly matched layer (PML) technique [17] is also adopted when the electromagnetic fields and adjoint variables were analyzed.

II. Mathematical Formulation and Analysis

Let us consider the scatterers of an arbitrary bounded cross section (Fig. 1). The domain of the scatterers (D) is illuminated by plane waves, which are polarized in the z-direction. To reconstruct the unknown complex permittivity distribution of scatterers in the objective domain, it is necessary to minimize the difference between the calculated scattered fields and measured ones. To evaluate such a difference, the error or objective function is defined as

$$F = \frac{1}{2}\sum_{i}^{N_T}\sum_{j}^{N_R}\int_0^{T_f}\left\{E_c^s(t)|_{ij} - E_m^s(t)|_{ij}\right\}^2 dt \qquad (1)$$

where N_T is the number of transmitters, N_R is the number of receivers, and T_f is the fixed final time. E_m^s is the measured scattered field and E_c^s is the calculated one at the measuring point.

Applying the first variation to (1) with respect to the inversion variable vector $\{p\}$, the derivatives of error function can be obtained as

$$\frac{dF}{d\{p\}} = \frac{1}{2}\sum_{i}^{N_T}\sum_{j}^{N_R}\int_0^{T_f}\frac{\partial G_{ij}}{\partial\{p\}} + \frac{\partial G_{ij}}{\partial\, E_c^s|_{ij}}\frac{\partial\, E_c^s|_{ij}}{\partial\{p\}}dt \qquad (2)$$

where $G_{ij} = \left(E_c^s|_{ij} - E_m^s|_{ij}\right)^2$

In general, the scattered field variable E_c^s has an implicit relationship with the variables $\{p\}$, and $dF/d\{p\}$ can be obtained using an indirect method. To reduce the computing time, the adjoint-variable method is introduced.

A. DSA Based on FETD

When the FDTD technique is used in the inversion process, the design sensitivity cannot be obtained directly because the adjoint-variable equation in the FDTD algorithm cannot be derived in a straightforward manner, while that in FEM can be. Therefore, an adjoint-variable equation that is derived from system matrices of the finite-element time-domain (FETD) formulation is employed. This adjoint-variable equation is then transformed as the coupled Maxwellian curl equations.

From the Maxwell's equations, the 2-D TM^z scalar wave equation can be derived, which is written as

$$\nabla^2 E_z - \frac{\varepsilon_r}{c_0^2}\frac{\partial^2 E_z}{\partial t^2} - \mu_0\sigma\frac{\partial E_z}{\partial t} = \mu_0\frac{\partial J_z}{\partial t} \qquad (3)$$

where ε_r denotes the relative permittivity, σ denotes the conductivity, c_0 denotes the velocity of light in free space, and J_z denotes the impressed electric-current density. In this algorithm, the direct problem is solved by the FDTD technique. The electromagnetic fields can be calculated without spurious solutions. Therefore, the vector basis function is not needed to calculate the sensitivity information. Applying the nodal element and Galerkin's formula to (3), this equation can be discretized and the matrix equation can be constructed as

$$[K]\{e_z\} + [M]\{\ddot{e}_z\} + [B]\{\dot{e}_z\} = \{Q\} \qquad (4a)$$

$$e_z(0) = 0 \qquad (4b)$$

$$\dot{e}_z(0) = 0 \qquad (4c)$$

where the dot denotes the time derivative and e_z is the z-direction component of the electric field at the node in the 2-D TM^z grid. The elemental matrices and load vector of (4) contain the integral of the following:

$$K_{ij}^e = \int_{\Omega^e}\nabla N_i\nabla N_j d\Omega^e \qquad (5a)$$

$$M_{ij}^e = \frac{1}{c_0^2}\int_{\Omega^e}\varepsilon_r^e N_i N_j d\Omega^e \qquad (5b)$$

$$B_{ij}^e = \mu_0\int_{\Omega^e}\sigma^e N_i N_j d\Omega^e \qquad (5c)$$

$$Q_i^e = -\mu_0\int_{\Omega^e} N_i\dot{J} d\Omega^e \qquad (5d)$$

where N_i is a nodal basis function of the grid. Using the adjoint variable λ, the adjoint equation of (4) can be derived as follows [12] :

$$[M]\{\ddot{\lambda}\} - [B]\{\dot{\lambda}\} + [K]\{\lambda\} = \left\{\frac{\partial G}{\partial E_c^s}\right\}^T \qquad (6)$$

subject to

$$\lambda(T_f) = \dot{\lambda}(T_f) = 0. \tag{7}$$

Equation (7) is the terminal condition on λ for solving (6). To deal with the terminal conditions, the backward time scheme $\tau = T_f - t$ is introduced. Equation (6) can be then converted into the initial-value problem. Using (2) and (6), the design sensitivity (2) can be transformed into

$$\frac{\partial F}{\partial \varepsilon_r} = \sum_i^{N_T} \sum_j^{N_R} \int_0^{T_f} \lambda^T \frac{\partial}{\partial \varepsilon_r} R(t, \varepsilon_r, \sigma) dt \tag{8a}$$

$$\frac{\partial F}{\partial \sigma} = \sum_i^{N_T} \sum_j^{N_R} \int_0^{T_f} \lambda^T \frac{\partial}{\partial \sigma} R(t, \varepsilon_r, \sigma) dt \tag{8b}$$

where

$$R(t, \varepsilon_r, \sigma) = \{Q\} - [M]\left\{\tilde{\ddot{e}}_z\right\} - [B]\left\{\tilde{\dot{e}}_z\right\} - [K]\{\tilde{e}_z\}. \tag{9}$$

The notation $\sim$ indicates that the argument is held constant for the derivative process with respect to ε_r and σ. Note that $[M]$ is the only matrix dependent on ε_r and $[B]$ is the only matrix dependent on σ.

B. DSA Based on FDTD

From the uniqueness theorem, (6) can be transformed into the Maxwellian coupled curl equations as follows:

$$\frac{\partial \lambda^{E_z}}{\partial y} = -\frac{\partial \lambda^{B_x}}{\partial t} \tag{10a}$$

$$\frac{\partial \lambda^{E_z}}{\partial x} = \frac{\partial \lambda^{B_y}}{\partial t} \tag{10b}$$

$$\frac{\partial \lambda^{Hy}}{\partial x} - \frac{\partial \lambda^{Hx}}{\partial y} - \sigma \lambda^{E_z} = \frac{\partial \lambda^{D_z}}{\partial t} + J_z^{\lambda} \tag{10c}$$

subject to

$$\lambda^{E_z}(T_f) = \lambda^{H_x}(T_f) = \lambda^{H_y}(T_f) = 0. \tag{11}$$

In addition, these adjoint-variable vectors satisfy the constitutive relation as the electromagnetic field vectors, i.e.,

$$\vec{\lambda}^D = \varepsilon \vec{\lambda}^E \tag{12}$$

$$\vec{\lambda}^B = \mu \vec{\lambda}^H. \tag{13}$$

In (6), J_z^{λ} is an infinitesimal pseudoelectric current element. Consequently, this pseudocurrent density is not an exact source of the FDTD scheme

$$\left.\frac{\partial G}{\partial E_z}\right|_{\Omega_m} = \mu_0 \int_{\Omega_m} N_i \dot{j}_z^{\lambda} d\Omega. \tag{14}$$

In order to apply J_z^{λ} to the FDTD solver, the FDTD pseudocurrent density can be represented as follows [18]:

$$J_z^{\lambda}(x, y, t) = J_z^{\lambda}(t) \delta(x - x_m, y - y_m). \tag{15}$$

By inserting (15) into (14) and assuming that the grid is a square quadrilateral, the right-hand side of (14) can be written as

$$\mu_0 \int_{\Omega_m} N_i \dot{j}_z^{\lambda} d\Omega = \mu_0 \dot{j}_z^{\lambda} \Delta \tag{16}$$

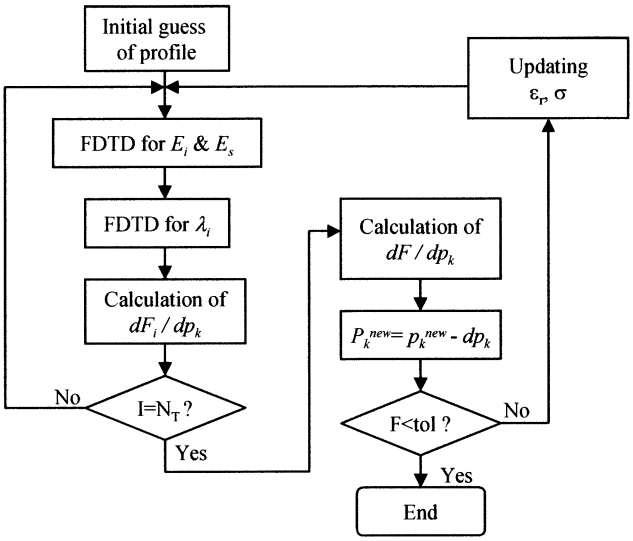

Fig. 2. Inversion algorithm using the FDTD technique. Geometry of mesh is fixed during all iteration.

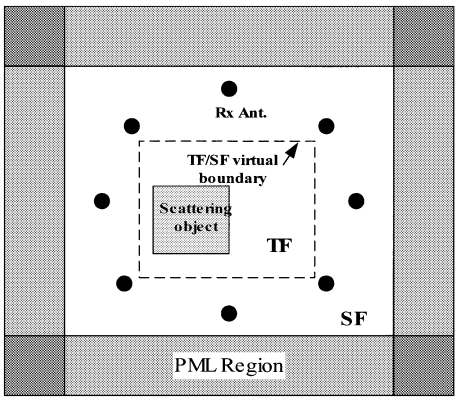

Fig. 3. Numerical configuration of problem. The TM^z plane wave is incident at each direction, and at each Rx Ant. position E_z field is measured.

where Δ is the area of the grid. Therefore, J_z^{λ} can be written as

$$J_z^{\lambda}(t) = \frac{1}{\mu_0 \Delta} \int_0^t \frac{\partial G(t')}{\partial e_z} dt'. \tag{17}$$

III. Topology Optimization

Most of the shape optimization techniques using the design sensitivity method have some difficulties in being applied to the inverse problems. This is because the topology of the design space should be given before the optimization and only the boundaries between the different materials are modified during the optimization process. This feature becomes a significant shortcoming in the inverse problems where there is no predetermined shape or topology. However, the topology optimization method does not require any preset shape or topology. The material property of each design cell in the whole design area is controlled simultaneously in each iteration step. Therefore, any shape or topology can be generated using this method. For these reasons, the topology optimization method is best suited for inverse problems.

In order to smoothly reconstruct the complex permittivity profiles, the topology optimization based on the normalized ma-

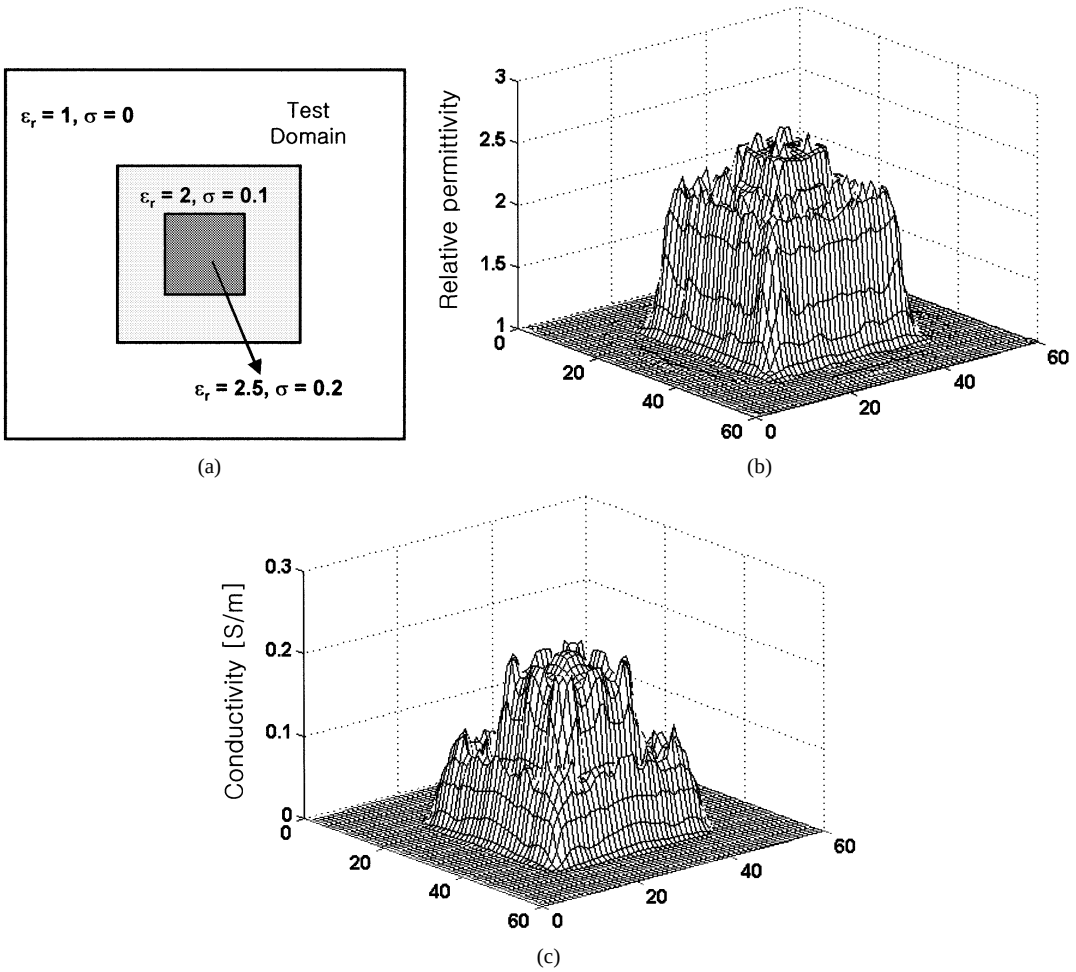

Fig. 4. Reconstruction of a single object in air after 100 iterations. (a) Original ε_r, σ shape. (b) Reconstructed ε_r. (c) Reconstructed σ.

terial density is introduced [15]. In the topology optimization, the test domain to be reconstructed is divided into small grids and the material composition of each grid is taken as the inversion variable. By controlling the material composition of each grid, the unknown object relative permittivity and conductivity can be reconstructed. The key concept of this method is to determine how to treat the material composition in order to estimate the objective function, and to reconstruct the final object shape. There are two methods for treating the material composition, homogenization method, and density method. The homogenization method provides the solid material a physical and mathematical basis for the calculation of the material properties of the composite or intermediate materials. On the other hand, the density method takes the material density of each grid as the design variable and is not concerned with the microstructure, but only with the results. In this paper, the density method is preferred.

To apply the density method to the reconstruction scheme, the normalized density vector of material $\{p\}$ is introduced, each of element p_i has a value between 0–1. Using the normalized density vector $\{p\}$, the complex permittivity can be represented as

$$\varepsilon_r(p_1) = (\varepsilon_{ro} - 1)\, p_1^h + 1, \qquad 0 < p_1 \leq 1 \tag{18a}$$

$$\sigma(p_2) = \sigma_o p_2^h, \qquad 0 < p_2 \leq 1 \tag{18b}$$

where ε_r is the relative permittivity of the real material in the test domain, σ is the conductivity of the real material in the test domain, p_i is the normalized density, which takes the value between 0–1, and h is the exponent that penalizes the intermediate density for faster convergence.

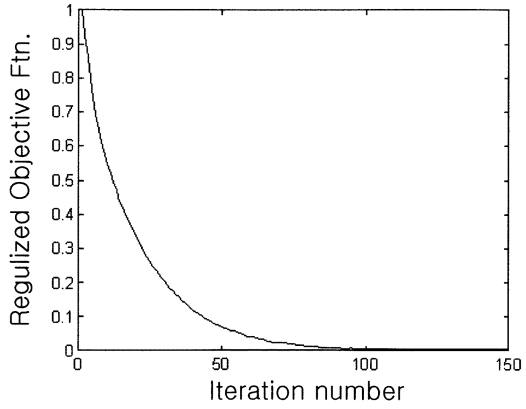

Fig. 5. Objective function value normalized by the initial value versus the iteration number when single object in air case reconstruction.

When h is larger, the intermediate density is more heavily penalized, which means it can be reconstructed more efficiently. However, larger values of h can also limit the design space at the same time. Usually, the value of h can be chosen between 2–4 by considering this tradeoff [19]. That is, if the intermediate density is not a significant problem and the user wishes to access

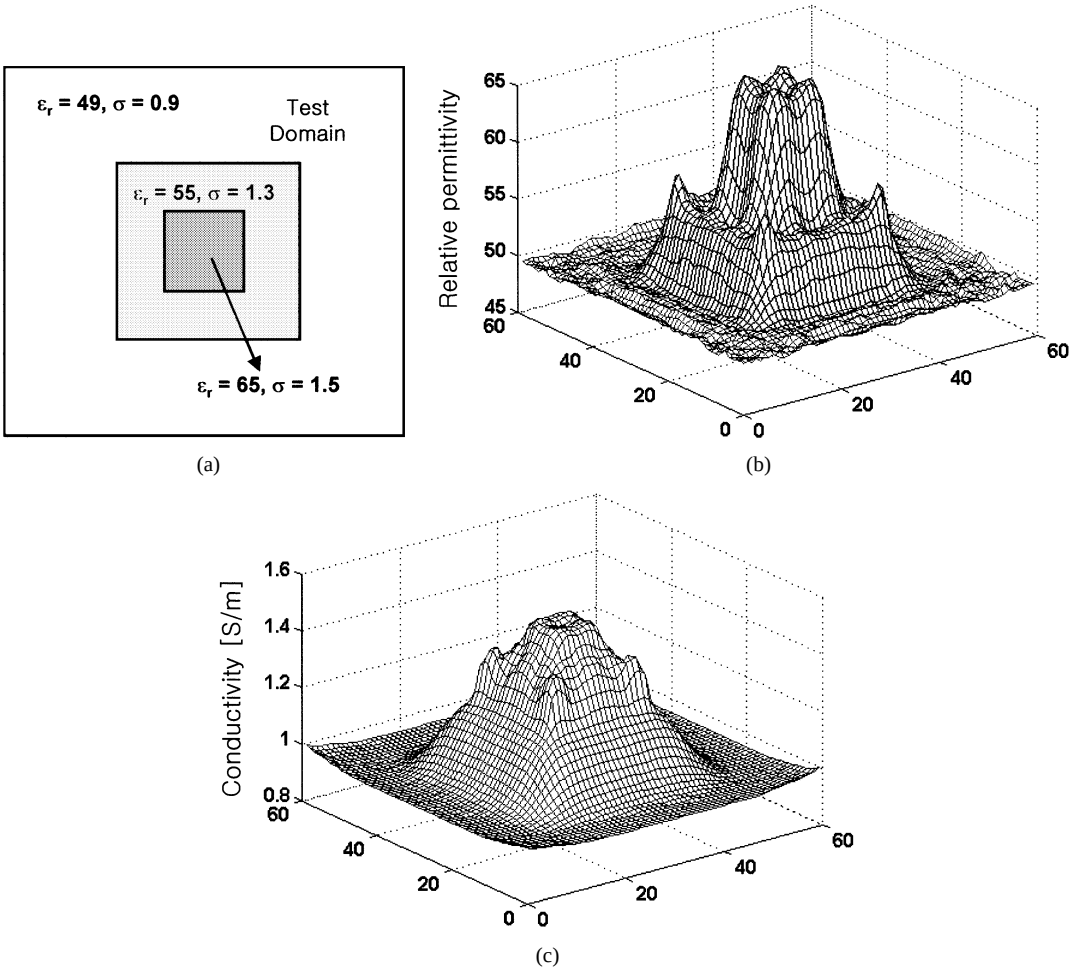

Fig. 6. Reconstruction of a single object in lossy medium after 245 iterations. (a) Original ε_r, σ shape. (b) Reconstructed ε_r. (c) Reconstructed σ.

a larger design space, $h = 2$ can be used. On the other hand, if the design space is sufficiently smooth and the intermediate material has a major difficulty in optimization, $h = 4$ should be used. For our case, $h = 2$ is selected because our problems has the abrupt change of profile. The normalized material density p is defined at each grid in the test domain. When p_1 is 0, it means the permittivity is that of air, and when p_1 is 1, the permittivity is that of a solid material. When p_2 is 0, it means the conductivity is that of air, and when p_2 is 1, the conductivity is that of a material that has an assumable maximum conductivity. p_i value between 0–1 corresponds to the intermediate material property. By inserting (18) into (8), one can rewrite the derivative error function F with respect to the normalized material density p as

$$\frac{\partial F}{\partial p_1} = h \sum_i^{N_T} \sum_j^{N_R} \int_0^{T_f} \lambda^T \frac{\partial}{\partial p_1} \left(-[M] \left\{ \tilde{\tilde{e}}_z \right\} \right) (\varepsilon_{ro} - 1) p_1^{h-1} dt \tag{19a}$$

$$\frac{\partial F}{\partial p_2} = h \sum_i^{N_T} \sum_j^{N_R} \int_0^{T_f} \lambda^T \frac{\partial}{\partial p_2} \left(-[B] \left\{ \tilde{\tilde{e}}_z \right\} \right) \sigma_o p_2^{h-1} dt. \tag{19b}$$

Equation (10a)–(10c) can then be also solved by using the FDTD technique with terminal conditions (11), and introducing the electric fields and adjoint variables solved by using the FDTD technique, one can also calculate the design sensitivity. Fig. 2 shows the inversion algorithm using the FDTD technique and design sensitivity.

IV. Numerical Examples

The efficiency of the proposed method is validated by means of three numerical 2-D examples. The unknown scatterers were assumed to lie entirely within total field region (TF in Fig. 3) of $L \times L$ square cells. Therefore, the total number of unknowns for inverse problem is $2^* L^2$. The standard Yee algorithm is used for the FDTD technique, and the geometry of the rectangular mesh is fixed during the entire iteration. The scatterers are illuminated by the TM^z plane waves with a Gaussian pulse from N_T different angles of incidence, uniformly distributed around the total field region. The scattered field is measured at N_R points lying on a circle centered in test domain and uniformly distributed around the scatterer for each illumination. The measurements are simulated by solving the direct problem.

The numerical configuration of the problem is shown in Fig. 3. In order to realize a plane-wave source, the total-field/scattered-field scheme is adopted. The incident wave is a Gaussian pulse modulated by a sine function with a center frequency of 5 GHz.

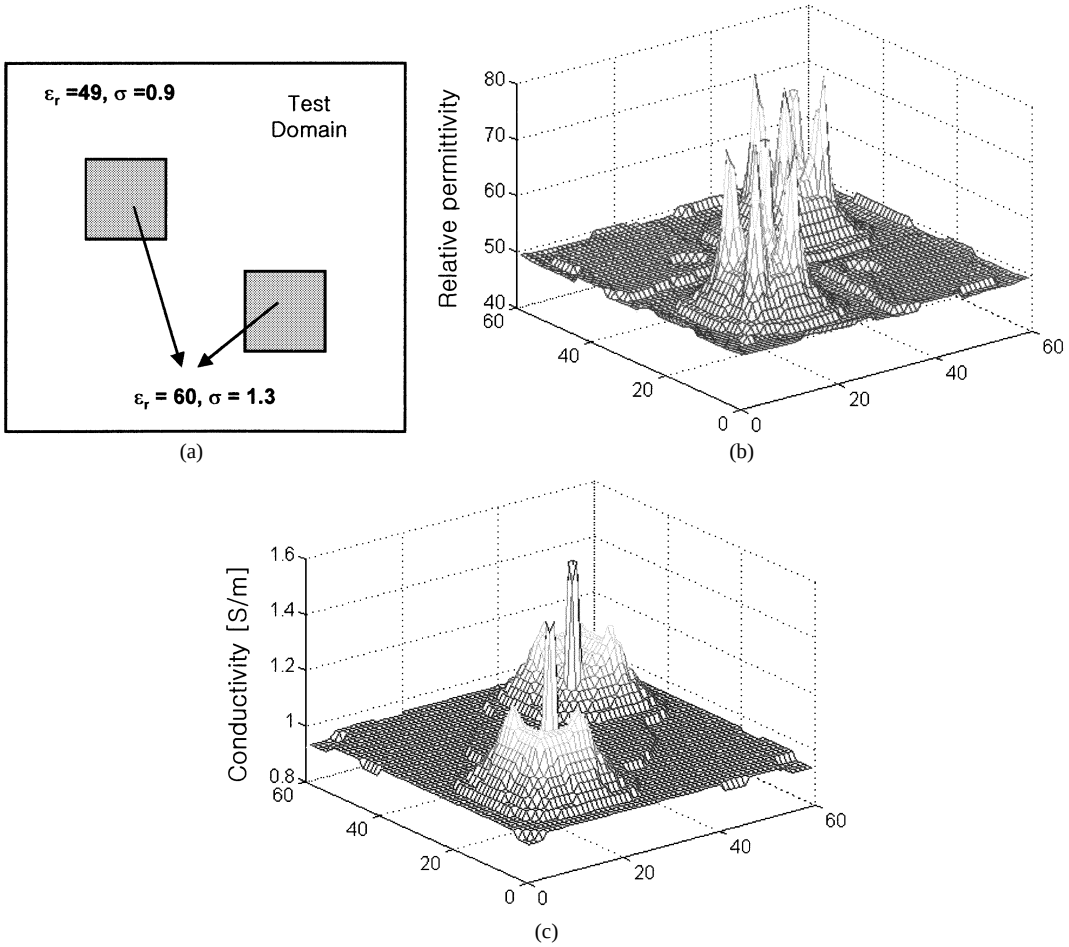

Fig. 7. Reconstruction result of multiple objects in lossy material after 100 iterations. (a) Original ε_r, σ shape. (c) Reconstructed ε_r. (d) Reconstructed σ.

A. Single Object in Air or Lossy Medium

As a first example, a lossy single scatterer of size $0.5\lambda \times 0.5\lambda$ in the $\lambda \times \lambda$ test domain is considered, where λ is the wavelength in the surrounding medium. The number of transmitters and receivers is 16 each. The measurement points are located in the scattered-field region (SF in Fig. 3) around the central point of the test domain. The number of grids in the test domain is 60 $\times$60. Fig. 4(a) shows the original ε_r and σ profile of the presented model. The medium is composed of two concentric square cylinders. The inner cylinder with $\varepsilon_r = 2.5, \sigma = 0.2$ is surrounded by a cylinder with $\varepsilon_r = 2.0, \sigma = 0.1$ and the other region is filled with air. The initial guess was that of surrounding material. Fig. 4(b) and (c) shows the reconstructed profiles, which are obtained after 100 iterations. Fig. 5 shows the values of the objective function normalized by the initial value as the iteration proceeds. After 100 iterations, the objective function value variation is less than 2%.

Another example of the single object reconstruction is showed in Fig. 6. The number of transmitters and receivers is the same as in the previous example. The inner cylinder with $\varepsilon_r = 65, \sigma = 1.5$ is surrounded by a cylinder with $\varepsilon_r = 55, \sigma = 1.3$, and the other region is filled with the lossy medium with $\varepsilon_r = 49, \sigma = 0.9$. Fig. 6 shows the original profiles and reconstructed results after 245 iterations. To reconstruct the profiles, an additional number of iterations is needed because of high permittivity of the surrounding medium.

TABLE I
CPU TIME FOR ONE INVERSE ITERATION

Single Object in Air		Multiple object in lossy material	
Routine	Time (s)	Routine	Time (s)
Field Analysis	48	Field Analysis	390
Adjoint Analysis	48	Adjoint Analysis	390
Sensitivity Analysis	12	Sensitivity Analysis	12

B. Multiple Objects in Lossy Medium

Another interesting problem is the reconstruction of multiple distinct scatterers surrounded by lossy material like water. As an example, two lossy scatterers are considered in the $\lambda \times \lambda$ test domain. Each object has a size of $0.25\lambda \times 0.25\lambda$. The number of transmitters and receivers is 32, and the number of grids in the test domain is 60 $\times$ 60. Fig. 7(a) shows the original ε_r and σ of the presented model. Two cylinders with $\varepsilon_r = 60$, $\sigma = 1.3$ are surrounded by a lossy material with $\varepsilon_r = 49.0$, $\sigma = 0.9$. Fig. 7(b) and (c) shows the reconstructed profiles that are obtained after 100 iterations. After 100 iterations, the position of each object can be detected correctly, but the profiles of the relative permittivity and conductivity showed some variation at the corner point of the object.

Table I represents the computational time that is measured on an 800-MHz Pentium III personal computer (PC). The CPU time of the sensitivity analysis is relatively small compared with

that of the field or adjoint analysis, and the CPU time of the field analysis is nearly equal to that of the adjoint analysis. For the lossy surrounding material, the time step is significantly reduced to meet the stability condition of the FDTD technique.

V. Conclusion

A numerical 2-D reconstruction algorithm for microwave imaging in the TM^z case has been presented. The algorithm utilizes the FDTD, DSA, and topology optimization technique. Using the adjoint-variable method, the design sensitivity is obtained by only two simulations at each design process, regardless of the number of design variables.

The method has been applied to the scattering objects illuminated by the pulse-type wave source. Using the proposed method, lossy dielectric objects surrounded by air or immersed in a lossy medium with a high permittivity have been successfully reconstructed in both the dielectric constant and electric conductivity.

References

[1] W. C. Chew, *Waves and Fields in Inhomogeneous Media*. New York: Van Nostrand, 1990.

[2] H. Harada, D. J. N. Wall, T. Takenaka, and M. Tanaka, "Conjugate gradient method applied to inverse scattering problems," *IEEE Trans. Antennas Propagat.*, vol. 43, pp. 784–792, Aug. 1995.

[3] R. E. Kleinman and P. M. van den Berg, "A modified gradient method for two-dimensional problems in tomography," *J. Comput. Appl. Math.*, vol. 42, pp. 17–35, 1992.

[4] S. Barkeshli and R. G. Lautzenheiser, "An iterative method for inverse scattering problems based on an exact gradient search," *Radio Sci.*, vol. 29, no. 4, pp. 1119–1130, July–Aug. 1994.

[5] R. E. Kleinman and P. M. van den Berg, "Two-dimensional location and shape reconstruction," *Radio Sci.*, vol. 29, no. 4, pp. 1157–1169, July–Aug. 1994.

[6] I. T. Rekanos, T. V. Yioultsis, and T. D. Tsiboukis, "Inverse scattering using the finite-element method and a nonlinear optimization technique," *IEEE Trans. Microwave Theory Tech.*, vol. 47, pp. 336–344, Mar. 1999.

[7] K. D. Paulsen, P. M. Meaney, M. J. Moskowitz, and J. M. Sullivan, Jr., "A dual mesh scheme for finite element based reconstruction algorithms," *IEEE Trans. Med. Imag.*, vol. 14, pp. 504–514, Sept. 1995.

[8] W. C. Chew, "Imaging and inverse problems in electromagnetics," in *Advances in Computational Electrodynamics: The Finite-Difference Time-Domain Method*, A. Taflove, Ed. Norwood, MA: Artech House, 1998, ch. 12.

[9] F.-C. Chen and W. C. Chew, "Time-domain ultra-wideband microwave imaging radar system," in *Proc. IEEE Instrum. Meas. Conf.*, 1998, pp. 648–650.

[10] S. C. Hagness, A. Taflove, and J. E. Bridges, "Two-dimensional FDTD analysis of a pulsed microwave confocal system for breast cancer detection: Fixed-focus and antenna-array sensors," *IEEE Trans. Biomed. Eng.*, vol. 45, pp. 1470–1479, Dec. 1998.

[11] ——, "Three-dimensional FDTD analysis of a pulsed microwave confocal system for breast cancer detection: Design of an antenna-array element," *IEEE Trans. Antennas Propagat.*, pp. 783–791, May 1999.

[12] Y.-S. Chung, C. Cheon, I. H. Park, and S. Y. Hahn, "Optimal shape design method for microwave device using time domain method and design sensitivity analysis," *IEEE Trans. Microwave Theory Tech.*, vol. 48, pp. 2289–2296, Dec. 2000.

[13] ——, "Optimal shape design of dielectric structure using FDTD and topology optimization," in *IEEE MTT-S Int. Microwave Symp. Dig.*, vol. 3, May 2000, pp. 2063–2066.

[14] E. J. Haug, K. K. Choi, and V. Komkov, *Design Sensitivity Analysis of Structural Systems*. New York: Academic, 1986.

[15] J. K. Byun, I. Park, H. Lee, K. Choi, and S. Hahn, "Inverse problem application of topology optimization method with mutual energy concept and design sensitivity," *IEEE Trans. Magn.*, vol. 36, pp. 1144–1147, July 2000.

[16] A. Taflove, *Computational Electrodynamics: The Finite-Difference Time Domain Method*. Norwell, MA: Artech House, 1995.

[17] J. Berenger, "A perfectly matched layer for the absorption of electromagnetic waves," *J. Comput. Phys.*, vol. 114, pp. 185–200, 1994.

[18] D. N. Buechler, D. H. Roper, C. H. Durney, and D. A. Christensen, "Modeling sources in the FDTD formulation and their use in quantifying source and boundary condition errors," *IEEE Trans. Microwave Theory Tech.*, vol. 43, pp. 810–814, Apr. 1995.

[19] R. J. Yang, "Multidiscipline topology optimization: A new microstructure-based design domain method," *Comput. Structures*, vol. 61, no. 5, pp. 1205–1212, 1997.

No-Weon Kang was born in Deajeon, Korea, in 1968. He received the B.S. and M.S. degrees in electrical engineering from the Seoul National University, Seoul, Korea, in 1991 and 1994, respectively, and is currently working toward the Ph.D. degree at Seoul National University.

From 1994 to 1999, he was with LG Industrial Systems (LGIS). His current research is focused on the numerical inversion technique, design and analysis of millimeter-wave passive devices, and electromagnetic interference (EMI)/electromagnetic compatibility (EMC) problem.

Young-Seek Chung (A'01–M'01) received the B.S., M.S., and Ph.D. degrees in electrical engineering from the Seoul National University, Seoul, Korea, in 1989, 1991, and 2000, respectively.

From 1991 to 1996, he was with the Living System Laboratory, LG Electronics. From 1998 to 2000, he was a Teaching Assistant of electrical engineering at the Seoul National University. Since 2001, he has been with Syracuse University, Syracuse, NY, where he is currently a Post-Doctoral Fellow. His current interests are numerical analysis using time-domain methods and the inverse scattering problem.

Changyul Cheon (S'87–M'90) was born in Seoul, Korea, on April 5, 1960. He received the B.S. and M.S. degrees in electrical engineering from the Seoul National University, Seoul, Korea, in 1983 and 1985, respectively, and the Ph.D. degree in electrical engineering from The University of Michigan at Ann Arbor, in 1992.

From 1992 to 1995, he was with the Department of Electrical Engineering, Kangwon National University, Chuncheon, Korea, as a Assistant Professor. He is currently an Associate Professor of electrical engineering with the Department of Electronics, University of Seoul, Seoul, Korea, where his group is currently involved with the design and analysis of microwave and millimeter-wave passive device using FEM, FDTD, and MoM techniques. He is also interested in high-power microwave systems for military and commercial applications.

Hyun-Kyo Jung (S'82–M'90–SM'99) received the B.S., M.S., and Ph.D. degree in electrical engineering from the Seoul National University, Seoul, Korea, in 1979, 1981 and 1984, respectively.

From 1985 to 1994, he was a member of the faculty with Kangwon National University. From 1987 to 1989, he was with the Polytechnic University of Brooklyn, Brooklyn, NY. From 1999 to 2000, he was a Visiting Professor with the University of California at Berkeley. He is currently a Professor with the School of Electrical Engineering and Computer Science/Electrical Engineering, Seoul National University. His research interests are various fields of the analysis and design of electric machines and numerical analysis of electrical systems, especially with the FEM.